

Modeling Precipitation Extremes using Log-Histospline

Whitney K. Huang*, Douglas W. Nychka†, Hao Zhang‡

September 21, 2022

Abstract

One of the commonly used approaches to modeling univariate extremes is the peaks-over-threshold (POT) method. The POT method models exceedances over a (sufficiently high/low) threshold as a generalized Pareto distribution (GPD). This method requires the selection of a threshold that might affect the estimates. Here we propose an alternative method, the “Log-Histospline (LHSpline)”, to explore modeling the tail behavior and the remainder of the density in one step using the full range of the data. LHSpline applies a smoothing spline model to a finely binned histogram of the log transformed data to estimate its log density. By construction, a LHSpline estimation is constrained to have polynomial tail behavior, a feature commonly observed in geophysical observations. We illustrate LHSpline method by analyzing precipitation data collected in Houston, Texas.

1 Introduction

Estimating extreme quantiles is crucial for risk management in a variety of applications. For example, an engineer would seek to estimate the magnitude of the flood event which is exceeded once in 100 years on average, the so-called 100 year return level, based on a few decades of time series (Katz et al., 2002). A financial analyst needs to provide estimates of the Value at Risk (VaR) for a given portfolio, essentially the high quantiles of financial loss (Embrechts et al., 1997). In climate change studies, as the research focus shifts from estimating the global mean state of climate variables to the understanding of

*Statistical and Applied Mathematical Sciences Institute. E-mail: whuang@samsi.info

†Institute for Mathematics Applied to Geosciences, Computational and Information Systems Laboratory, National Center for Atmospheric Research. E-mail: nychka@ucar.edu

‡Department of Statistics, Purdue University. E-mail: zhanghao@purdue.edu

regional and local climate extremes, there is a pressing need for better estimation of the magnitudes of extremes and their potential changes in a changing climate (Zwiers and Kharin, 1998; Cooley et al., 2007; Kharin et al., 2007; AghaKouchak et al., 2012; Shaby and Reich, 2012; Kharin et al., 2013; Huang et al., 2016).

The estimation of extreme quantiles poses a unique statistical challenge. In general, extreme quantile estimation requires an estimate of the upper tail of a distribution, but typically the available data provides little direct information (e.g. see Fig. 1). As a result, the estimate will have a large variance that can increase rapidly as we move progressively to high quantiles. Furthermore, if the quantile being estimated is beyond the range of data, the need to explicitly model the tail with some parametric form is unavoidable. This work presents a new statistical method, the “Log-Histospline (LHSpline)”, for estimating probabilities associated with extreme values. Our LHSpline method is consistent with extreme value theory and does not impose a parametric form where the density can be determined from the data. Its primary advantage is that it automates the fitting of distributions and so leads itself to mining large geophysical data sets. This is in contrast to more traditional extreme value theorem based methods that require some user intervention for fitting (see the next three paragraphs).

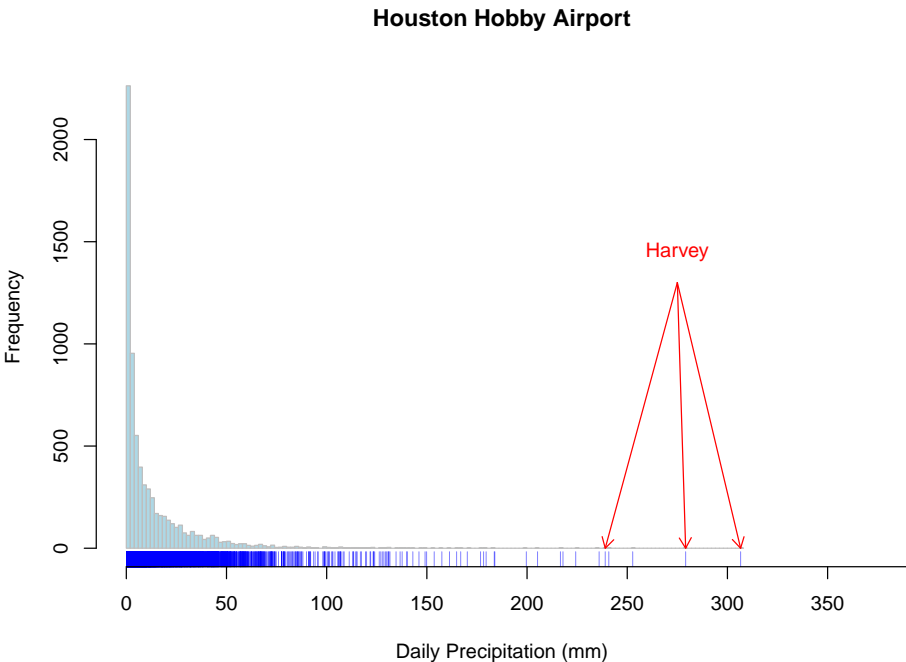


Figure 1: Histogram of daily rainfall amount (mm) at Hobby Airport in Houston, Texas from 1949 to 2017. The vertical ticks at the x-axis are the values of the individual data points. Due to its tail heaviness, the largest values are substantially larger than the bulk of the distribution. Three out of the five largest precipitation measurements were observed during Hurricane Harvey.

The development of extreme value theory (EVT) provides a mathematical framework of performing analysis and inference for extreme events. Two fundamental and connected results in EVT are based on asymptotic distributions of two kinds of data, namely, block maxima and peaks over threshold and are unified into a single family of distribution, the so-called *generalized extreme value* (GEV) distribution (Jenkinson, 1955). The reader is referred to Gumbel (1958) and Coles (2001) for more details.

One drawback of the block maxima (BM) method is that data are not used efficiently, that is, the sample size of the block maxima is n/b , which is substantially smaller than the original sample size n given that b need to be sufficiently large. Moreover, the top few largest order statistics within a given block should, in principle, inform us about the behavior of extreme events. The peak-over-threshold (POT) method is based on the

Picklands–Balkema–de Haan theory (Pickands, 1975; Balkema and De Haan, 1974), which establishes that the limiting distribution of the threshold exceedances (i.e. $[Y - u | Y > u]$ ¹ where Y denotes the random variable of interest and u a threshold) converges to the so-called *generalized Pareto distribution* (GPD) as the threshold u tends to the upper limit point $y_F = \sup\{y : F(y) < 1\}$. The POT method models exceedances over a (sufficiently high/low) threshold as a generalized Pareto distribution (GPD) (Smith, 1984; Davison, 1984; Davison and Smith, 1990). One advantage of the POT method over the BM method is that it typically makes use of the available data more efficiently in estimating extreme events.

To apply the POT method, a threshold u has to be chosen and the estimates may be sensitive to the chosen threshold (Scarrott and MacDonald, 2012; Wadsworth and Tawn, 2012). The threshold selection involves a bias-variance trade-off: if the chosen threshold is too high, the estimates exhibit large variability; if the chosen threshold is too low, the asymptotic justification of the GPD approximation to the tail density will be less effective, which leads to bias. There are several graphical tools that aim to help with the threshold selection, for example, the mean residual life plot and the parameter stability plot (e.g. Coles, 2001, p.80 and p.85). However, the use of these graphical tools can be quite challenging to choose an the appropriate threshold and is difficult (see Fig. 9 in Sec. 4 for an example) and automated selection is an active research problem (Dupuis, 1999; Wadsworth and Tawn, 2012). Another limitation of the POT method is that once the threshold has been chosen, there is no attempt to model the distributional behavior below the chosen threshold, which can be of interest in many applications.

Recently, there are some attempts to model the distribution of a random variable while retaining a GPD tail behavior (Frigessi et al., 2002; Tancredi et al., 2006; Carreau and Bengio, 2009; Papastathopoulos and Tawn, 2013; Naveau et al., 2016). These methods

¹We use Gelfand and Smith (1990)'s bracket notation for a distribution

can be broadly divided into two categorizes: the extreme value mixture model (see Scarrott and MacDonald, 2012; Dey and Yan, 2016 for review) and the *extended generalized Pareto distribution* (EGPD) method (Papastathopoulos and Tawn, 2013; Naveau et al., 2016). The basic idea of the extreme value mixture model is to model a distribution as a mixture of a *bulk* distribution and a GPD distribution above a threshold. This then adds the threshold as an another parameter to be estimated. However, the specification of the bulk distribution can have a nonnegligible impacts on the estimates of GPD parameters. This then can substanitally bias the tail estimates. Finally, the estimation uncertainty for the threshold can be quite large (Frigessi et al., 2002) and hence it is not clear whether this quantity can be identifiable. The extended Pareto method proposed by Papastathopoulos and Tawn (2013) bypasses this issue of the mixture modeling by proposing several classes of parametric models with GPD limiting behavior for the upper tail. Naveau et al. (2016) extended the scope of this approach by allowing the classes of parametric models with GPD limiting behavior for both lower and upper tails in an application to rainfall modeling.

In this work we propose a statistical method, the “Log-Histospline (LHSpline)”, that shares some commonalities with Naveau et al. (2016) but with additional flexibility in modeling the bulk of a distribution. This new method makes use of spline smoothing to represent the log-density in the bulk of the distribution and seamless transition to polynomial tail behavior where the data is sparse. Our motivating example is extreme precipitation modeling in the context of climate science. We would like to (i) provide a flexible model to the *full range* of the non-zero rainfall distribution and (ii) reliably estimate extreme events (e.g. 100-year daily rainfall amount). Our approach is to first log transform the data and then apply a generalized cubic smoothing spline on a finely binned histogram to estimate the log-density. The purpose of the data transformation step is similar to that of variable bandwidth in a density estimation literature (Wand et al., 1991) and a spline smoothing log-density estimation (Silverman, 1982) applied to

the transformed variable will ensure the algebraic (i.e. power-law) upper tail behavior, commonly observed in daily rainfall data. The LHSpline method enjoys flexible modeling in the bulk of distribution compared with the extended Pareto approach while the logarithm transformation and the linear extrapolation property of the natural cubic spline smoother ensures the algebraic tail structure where data is rare (see Section 2 for details).

The *Logspline* proposed by Kooperberg and Stone (1991) also uses a cubic spline to estimate the log-density of a distribution. By default a log transformation is not presupposed so this estimator enforces exponential tails beyond the spline knots. A salient difference between LHSpline and Logspline is that the Logspline method is under the framework of *regression spline* in that it chooses a small number and locations of k knot points. Once the knots are chosen, Logspline is essentially a parametric model.

Although we do not recommend that any statistical method be used in an automatic and black box way, our method can be applied with minimal choices and so is amenable to interpreting large climate related data sets and fitting many individual distributions. For example, the LHSpline could be used to summarize the distributions of precipitation in each grid cell from a high resolution and/or ensemble climate model experiment (e.g. Mearns et al., 2009; Wang and Kotamarthi, 2015). The resulting log-densities would then be amenable to extremes analysis and further dimension reduction across spatial scales and other covariates. In this mode we view the LHSpline as being a core tool within climate informatics.

The rest of this paper is structured as follows: In Section 2, we introduce the LHSpline and discuss its computation. A simulation study is presented in Section 3. An application to daily precipitation collected in Houston Hobby Airport, Texas is illustrated in Section 4. Finally, we conclude with a discussion and outline some future directions.

2 The Log-Histospline

2.1 The Model of Log Density: Natural Cubic Spline

Let Y be a continuous random variable with probability density function (pdf) $f(y)$.

Suppose Y is heavy-tailed:

$$f(y) \sim y^{-(\alpha+1)} \text{ as } y \rightarrow y_F, \quad \alpha > 0. \quad (1)$$

Without loss of generality we assume that $Y \in (0, \infty]$. Instead of modeling Y , we model $X = \log(Y)$, the logarithmic transformation of the original variable, via its log-density. That is, the pdf of X takes the following form:

$$e^{g_\alpha(x)}, \quad x \in (-\infty, \infty] \quad (2)$$

The log-density g completely specifies the distributional properties of Y (see eq. (3)). Moreover, modeling the log-density conveniently enforces the positivity constraint (Leonard, 1978; Silverman, 1982; Kooperberg and Stone, 1991; Eilers and Marx, 1996). The main idea is that we do not want to impose a strong parametric structure on g . This is similar to some approaches in nonparametric density estimation literature (see Silverman, 1986 for a comprehensive review). However, it is well-known that the usual nonparametric density estimation procedure will often introduce spurious features in the tail of the density due to limited information in the tail (e.g. Kooperberg and Stone, 1991). This issue is amplified when dealing with heavy-tailed distributions that are typically observed in precipitation data. On the other hand, since the focus is on estimating extreme quantiles, it is critical that the model can capture both qualitative (polynomial decay) and quantitative (the tail index α) behaviors of the tail density. We assume that g belongs to the family of *natural cubic splines* (see Definition 1) to accommodate both a flexible bulk distribution and the algebraic tail. Here we combine the ideas of *spline smoothing* (e.g. Wahba, 1990; Gu, 2013) and *Histospline* (Boneva et al., 1971) to derive an estimator.

Definition 1 (Natural cubic spline) A natural cubic spline $g(x)$, $x \in [a, b]$ is defined with a set of points $\{x_i\}_{i=1}^N$ such that $-\infty \leq a \leq x_1 \leq x_2 \leq \dots \leq x_N < b \leq \infty$ with the following properties:

1. g is linear, $x \in [a, x_1]$, $x \in [x_N, b]$
2. g is a cubic polynomial, $x \in [x_i, x_{i+1}]$, $i = 1, \dots, N-1$
3. $g \in \mathcal{C}^2$, $x \in (a, b)$

where \mathcal{C}^k is the class of functions with k continuous derivatives

Typically the spline function is extrapolated linearly outside (a, b) using the polynomial forms at both endpoints.

The cubic spline smoother is widely used in nonparametric density estimation due to its flexibility (e.g. Silverman, 1986; Gu, 2013) and hence provides a flexible model for the bulk of the distribution. By a standard argument of transformation of random variables, the density of $Y = \log(X)$ takes the form:

$$f(y) = y^{-1} e^{g_\alpha(\log(y))}, \quad y > 0 \quad (3)$$

When $y \rightarrow \infty$, the tail density of Y is

$$\begin{aligned} f(y) &= y^{-1} e^{g_\alpha(\log(y))} = y^{-1} e^{-\alpha \log(y) + \beta} \\ &= y^{-1} e^{-\alpha \log(y)} e^\beta = C y^{-1} e^{-\alpha \log(y)} \\ &= C y^{-1} y^{-\alpha} = C y^{-(\alpha+1)} \end{aligned} \quad (3.4)$$

Therefore, by the linear boundary conditions on a cubic spline we automatically obtain the algebraic tail behavior.

Let Y_1, Y_2, \dots, Y_n be an *i.i.d.* random sample from a continuous random variable Y that exhibits algebraic tail behavior. Without loss of generality, we assume the support is on the positive real line (i.e. $Y \in (0, \infty]$). The functional estimation of g , the log-density function of the log transformed random variable $X = \log(Y)$, involves two steps: data binning to create a histogram object, and a generalized smoothing spline of the histogram. In what follows, it is useful (see Fig. 2 to illustrate these steps using a synthetic data set simulated from a EGPD (Naveau et al., 2016, p. 2757)). Some considerations when applying LHSpline to real data will be discussed in next section.

Data binning: we first bin the transformed data $\{X_i\}_{i=1}^n$ by choosing $N + 1$ equally spaced points as the break points $\{b_j\}$ to construct the corresponding histogram object (i.e. the histogram counts $\{Z_j\} = \#\{X_i : X_i \in [b_j, b_{j+1}]\}$). We set the knots associated with the spline to the bin midpoints: $x_j = (b_j + b_{j+1})/2$ Several remarks on data binning should be made here:

- (1) an equally spaced bin size in the log scale implies a variable bin size with the bin size becoming increasingly larger in the upper tail;
- (2) the number of bins should be “sufficiently” large for the Poisson assumption made in the next step justifiable;
- (3) the choice of the first and especially the last break points (i.e. b_1 and b_{N+1}) will have non-negligible impacts on tail estimation in our framework. We will choose them somehow smaller (larger) than the minimum $X_{(1)}$ (maximum $X_{(n)}$) of the log-transformed data, which is different than what typically done in constructing a histogram. We will defer the discussion on this to the next step.
- (4) We make the assumption that the number of bins is fine enough so that $\int_{b_i}^{b_{i+1}} e^g(x)dx$ is well approximated by $e^g(x_i)(b_{i+1} - b_i)$

Smoothing the histogram: we adapt a penalized approach (Good and Gaskins, 1971; Tapia, 1978; Green, 1994) to obtain a functional estimate of g as follows. First, we

assume $\{Z_j\}_{j=1}^N$ each follows a Poisson distribution² (Lindsey, 1974a,b; Eilers and Marx, 1996; Efron and Tibshirani, 1996) with log intensity \tilde{g}_j , $j = 1, \dots, N$, given that N is large enough so that the bin size is fine enough. Furthermore, we assume $\tilde{g}_j \approx \tilde{g}(x_j)$, i.e., we assume the Poisson log intensity at each bin represents the log intensity function (unnormalized log density function) evaluated at the midpoint of each bin. Hence we perform a penalized Poisson regression to the data pair $\{Z_j, x_j\}_{j=1}^N$ using a log link function and with a penalty term that penalizes the “roughness” of \tilde{g} . The estimate \tilde{g} is the unnormalized version of g can be obtained by solving the following minimization problem:

$$-\sum_{j=1}^N \{\tilde{g}(x_j)z_j - e^{\tilde{g}(x_j)} - \log(z_j)!\} + \lambda \left(\int_{x \in \mathbb{R}} (\tilde{g}''(x))^2 dx \right) \quad (4)$$

where λ is the smoothing parameter. Note that the first term in the objective function is the negative log likelihood for the histogram counts with a Poisson assumption, and the second term, the squared integral of the second derivative of \tilde{g} multiply by the smoothing parameter, is the penalty function. The solution of this optimization problem exists, is unique and for any fixed λ , the solution is a natural cubic spline (Green, 1994; Gu, 2013). The selection of the smoothing parameter λ plays the role of balancing the data fidelity of the Poisson regression fit to the histogram counts, as presented by the negative log-likelihood, and the “smoothness” of \tilde{g} , and is chosen by approximate cross validation (CV, see O’Sullivan, 1988 for more details). Note that the smoothness penalty will favor linear functions, precisely the algebraic tail behavior we want in the untransformed distribution.

As mentioned in the remark (3) of the previous step that the choice of b_1 and b_{N+1} play an important role in our penalized approach. The reason is that if one uses $X_{(1)}$ for b_1 and $X_{(n)}$ for b_{N+1} , as typically done in constructing a histogram, then one will likely introduce a “boundary effect” and hence produce unreliable tail estimates. Specifically,

² $\{Z_j\}_{j=1}^N$ has a *multinomial* distribution with parameters n and $\boldsymbol{\pi} = (\pi_1, \dots, \pi_N)$ where π_j is the probability that a random variable X falls into the j th bin. Here we consider $Z_j \stackrel{ind}{\sim} \text{Pois}(\gamma\pi_j)$, $j = 1, \dots, N$. The MLE of γ under the Poisson model follows $\hat{\gamma} = \sum_{j=1}^N Z_j = n$ and $\hat{\boldsymbol{\pi}}$ is equal to the MLE of $\boldsymbol{\pi}$ under the multinomial model.

under the usual histogram construction (i.e. $b_1 = X_{(1)}$, $b_{N+1} = X_{(n)}$) and a large number of bins, as in our setting, one will very likely observe “bumps” in the boundaries of the histogram. As a result, the cross validation will maintain the smoothness and tend to overestimate the slope near the boundary. Our solution to mitigate this bias is to extend the range of the histogram beyond the sample maximum/minimum so that some zero counts will be included at both ends. Note that zero counts are also part of the data when fitting Poisson regression because a Poisson random variable can take 0. In fact, one can think that the estimation procedure of the LHSpline as a discrete approximation to estimating the intensity function of an inhomogeneous Poisson process (Brown et al., 2004). In this regard, one should take into account the range (spatial window in spatial point process context) as part of the data. How far one should extend beyond the range of the data to remove the bias? In principle, one should add as many bins as possible to reflect that $X \in (-\infty, \infty]$. However, doing this will cause the cross-validation to fail when selecting the smoothing parameter. One way to decide how many bins to add is to exploit the fact that for any continuous random variable X :

$$\mathbb{P}(X_{\text{new}} > X_{(n)}) \stackrel{d}{\approx} \text{Exp}(1)/n \quad (5)$$

and

$$\mathbb{P}(X_{\text{new}} < X_{(1)}) \stackrel{d}{\approx} \text{Exp}(1)/n \quad (6)$$

where $X_{(1)}$ and $X_{(n)}$ are the smallest and the largest order statistics from a random sample $\{X\}_{i=1}^n$, $X_{\text{new}} \sim F_X$ a yet observed random variable, and $\text{Exp}(1)$ denotes the exponential distribution with rate parameter 1.

One can use the facts above to decide how many bins to add so that the tail probabilities are calibrated in a distributional sense. For example, one can keep adding zero counts beyond the range until the resulting estimate $\hat{\mathbb{P}}(X > x_{(n)}) \approx 1/n$. Finally we re-normalized the \tilde{g} to make the integral of $\int_{\mathbb{R}} e^g$ equal to one. Numerical integration is

used to approximate the integral within the data range and an analytic form is used for the density beyond the bin limits.

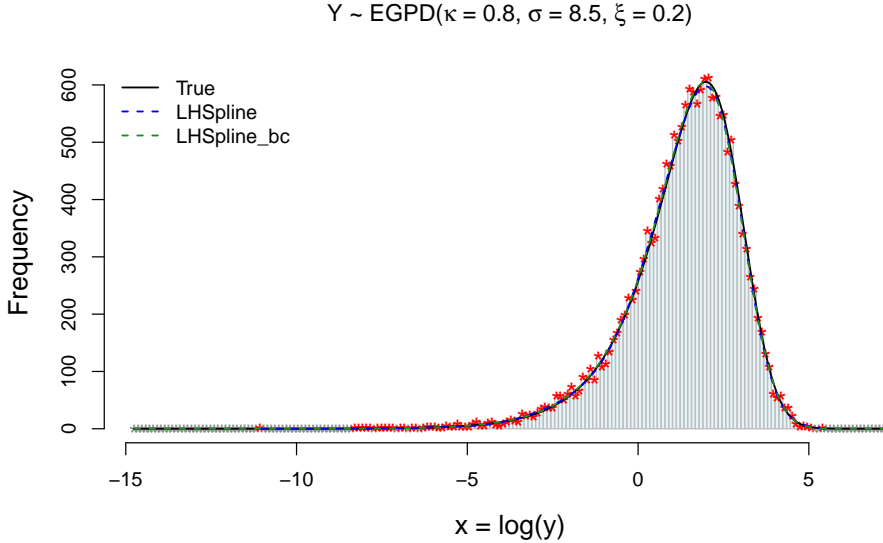


Figure 2: An illustration of applying LHSpline to a synthesis data. Here we bin the log transformed data $\{x_i\}_{i=1}^{18,250}$ into $N = 150$ equally-spaced intervals to obtain a histogram. Red asterisks denote the (non-zero) counts and gray asterisks denote (zero) counts. The LHSpline estimates with (without) boundary correction (green (blue) dashed line) are obtained by fitting a penalized Poisson regression to the histogram counts (both red and gray asterisks); the true density (the density of $X = \log(Y)$ where $Y \stackrel{i.i.d.}{\sim} \text{EGPD}(\kappa = 0.8, \sigma = 8.5, \xi = 0.2)$) is plotted as black solid line. Note that here we extend the range of the histogram to alleviate the boundary effect.

3 Simulation Study

The purposes of this simulation study is twofold: (i) to demonstrate how we implement the LHSpline to a synthetic data set and (ii) to compare LHSpline method with the EVT-based methods (i.e. POT and BM) in estimating extreme quantiles.

3.1 Setup

We simulate the data from the model (i) of the EGPD (see Naveau et al., 2016, p. 2757) with parameter values $\kappa = 0.8, \sigma = 8.5, \xi = 0.2$ and the sample size $n = 18,250$, which corresponds to a time series with 50 years of complete daily data (ignore the leaf year)

with 50 replications. The EGPD parameters are chosen to reflect a typical distributional behavior of daily precipitation.

3.2 LHSpline Illustration

We use one of the simulated data (see Fig. 2) to demonstrate the procedure of LHSpline as described in Sec. 2. To illustrate the “boundary effect” we first set equidistant breakpoints that span the whole range of the data, that is, $b_1 = x_{(1)}$, $b_{N+1} = x_{(n)}$, and $h = b_{i+1} - b_i = (x_{(n)} - x_{(1)})/N$, $i = 1, \dots, N$. We choose $N = 150$ meaning that we construct a histogram with a rather large number of bins (much larger than what the default in `hist` in R would suggest). We then apply the generalized smoothing spline procedure by solving the equation (4) via approximate cross-validation to obtain an estimate. Figure 3 shows the LHSpline estimate along with a GPD fit (with threshold u chosen as the .95 empirical quantile) and the true (log-density) density. Upon visual inspection one may conclude that LHSpline perform well, or at least as good as the POT, and both estimates are fairly close to the true one.

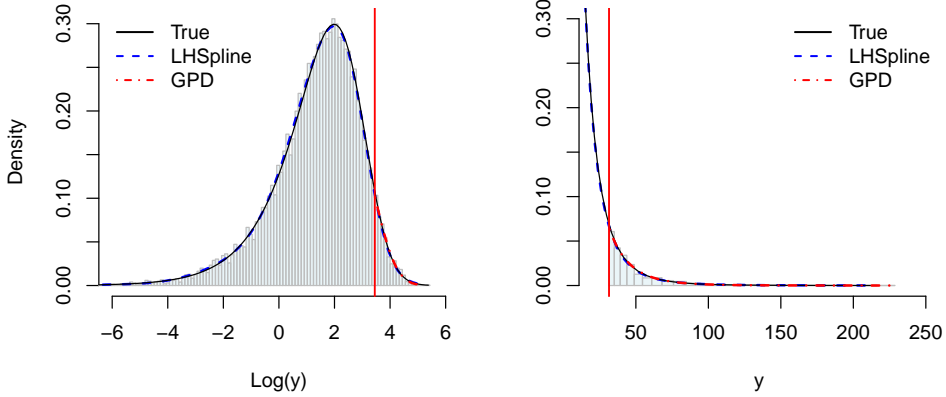


Figure 3: The density estimates for log scale X (**left**) and original scale Y (**right**). The blue dashed lines are the estimates obtained by LHSpline (without boundary correction), red dotdashes by POT with u as the .95 empirical quantile, and black underlying truth.

However, a more careful examination for the log-log plot (log-density against $\log(y)$) and the return levels estimation reveals that LHSpline with $b_1 = x_{(1)}$ and $b_{N+1} = x_{(n)}$, in general, overestimates the extreme quantiles (see Fig. 4).

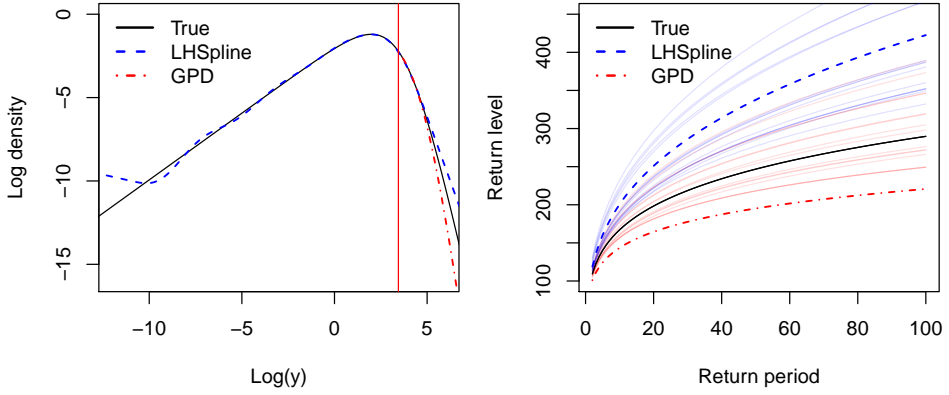


Figure 4: **Left:** Estimated log density against $\log(y)$. **Right:** Estimated return levels with return period ranging from 2 years to 100 years.

The issue of overestimation of LHSpline is largely due to the “boundary effect” when fitting penalized Poisson regression to a histogram. Specifically, the histogram counts in Fig. 2 are $\{Z_1 = 1, Z_2 = 0, \dots, Z_{25} = 0, Z_{26} = 1, \dots, Z_{149} = 0, Z_{150} = 1\}$. The histogram counts in the first and the last bins are non-zero (typically 1) by construction but the nearby bins are likely to be zero. Therefore, these “bumps” (see Fig. 5) at the both ends force the smoothing spline to overestimate the slopes. As a result, the LHSpline tends to over estimate the slopes at boundaries and hence the extreme quantiles.

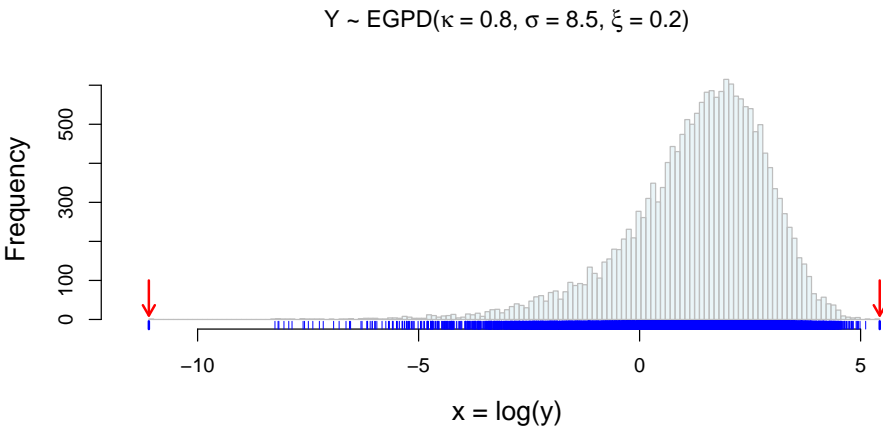


Figure 5: The issue of overestimation observed in Fig. 4 can be largely explained by the two isolated values ($x_{(1)}$ and $x_{(n)}$).

To alleviate this boundary effect, we apply a simple boundary correction by extending

one-third (with respect to 0) of the range of the histogram (see Fig. 2, this correction adds 33 (17) zero counts to the left (right) tail such that $\{\hat{\mathbb{P}}_{\text{LHSpline}}(X > x_{k,(n)})\}_{k=1}^{50} \stackrel{d}{\approx} \text{Exp}(1)/18250$ where $x_{k,(n)}$ denotes the sample maximum for the k th simulation) and refit this augmented data pairs (the original counts and those zero counts) to penalized Poisson regression. We observe that this strategy indeed removed the positive bias in the tail slope estimates in the log-density and hence removed the positive bias in return levels estimation (see Fig. 6).

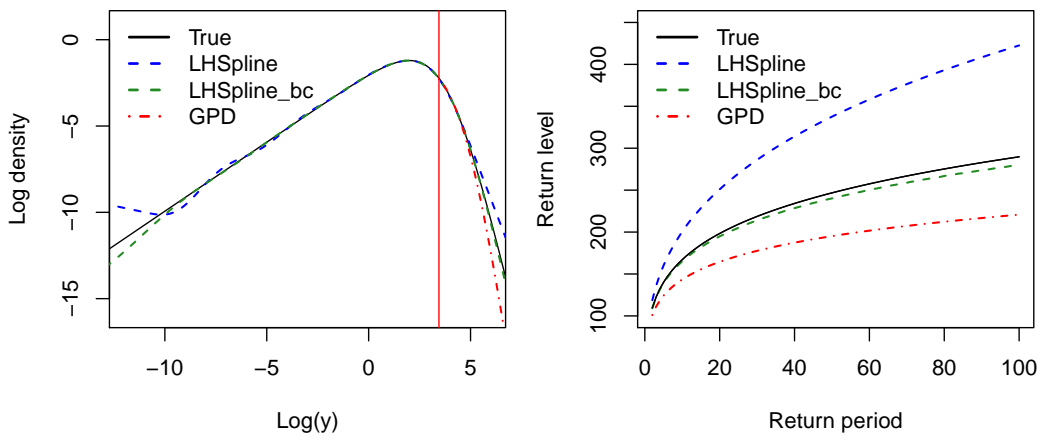


Figure 6: The estimated log density and return levels with (green dashed line) and without (blue dashed line) boundary correction. The estimates obtained by POT are shown in red dotdash line.

3.3 Comparison of Return Level Estimation

In this subsection we assess the performance of estimating high quantiles using LHSpline and two commonly used EVT-based methods, namely, the block maxima (BM) method by fitting a GEV to “annual maxima”, and the peaks-over-threshold (POT) method by fitting a GPD to excesses over a high threshold (.95 empirical quantile in our study). We estimate the GEV and GPD parameters using maximum likelihood and compare their plug-in estimates for 25-, and 100-year return levels with that of the LHSpline estimates (with and without boundary correction). To get a better sense of how well each method performs, we also include the “oracle estimates” where we fit the true model (EGPD) using maximum likelihood method to obtain the corresponding plug-in estimates.

Figure 7 shows that, perhaps not surprisingly, the variability of the return level estimates obtained by fitting threshold exceedances to a GPD distribution is generally lower than that of the estimates obtained by fitting block maxima to a GEV distribution under the *i.i.d.* setting here. Also, it is clear that the LHSpline without boundary correction can not only lead to serious bias but also inflate the estimation variance. After applying our boundary correction by expanding the data domain, the estimate becomes much closer to being unbiased with a substantial reduction in the estimation variability. Surprisingly, the estimation performance is very close to the estimates obtained from the oracle case.

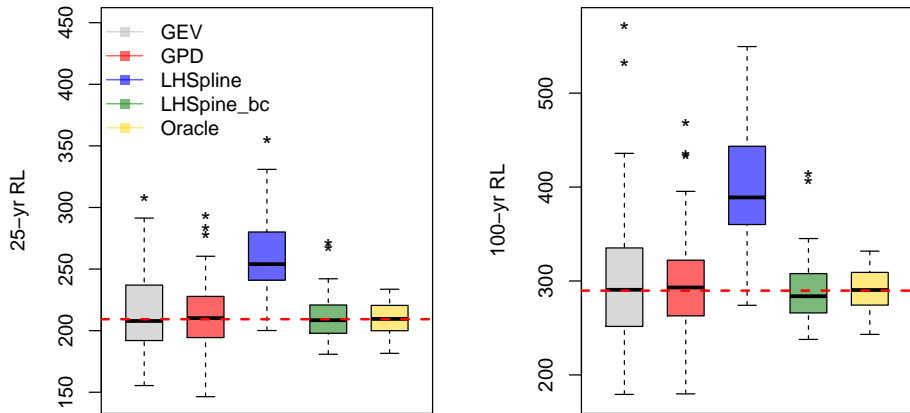


Figure 7: Boxplots of estimated **Left:** 25-, and **Right:** 100-year return levels using (from left to right in each panel) block maxima method (gray), peaks-over-threshold method (red), LHSpline with (green) and without (blue) boundary correction, and the true model (extended GP, oracle, golden). Boxplots are based on 50 independent replicates, and true values are represented by horizontal red dashed lines.

4 Applications

Between 25th and 31st August 2017 Hurricane Harvey brought unprecedented amounts of rainfall to the Houston metropolitan area, resulting in catastrophic damage to personal property and infrastructure. In the wake of such an extreme event, there is interest in understanding how the rarity of this event and how human-induced climate change might

alter the chances of observing such event (Risser and Wehner, 2017). In this section, we apply the LHSpline to the daily precipitation measurements in a weather station at Houston Hobby airport (see Fig. 1 for the histogram and Fig. 8 for the time series) from the Global Historical Climatology Network (GHCN).

4.1 Houston Hobby rainfall data set

The data used consisted of 69 years (1949 ~ 2017) daily precipitation observations at the Houston Hobby Airport weather station from the GHCN (see Fig. 8). To quantify to which degree the peak precipitation of the Hurricane Harvey at Hobby Airport was unusual. We fit a LHSpline with data prior to this event (from Jan. 1949 ~ Dec. 2016) to a 150 equal-spaced bins histogram to estimate the log-density for the full range of non-zero precipitation ($\sim 27.6\%$ of all the observations). To facilitate a comparison with POT method we also fit a GPD to excesses over a high threshold (chosen as .9 empirical quantile of nonzero daily precipitation, see diagnostic plot in Fig. 9).

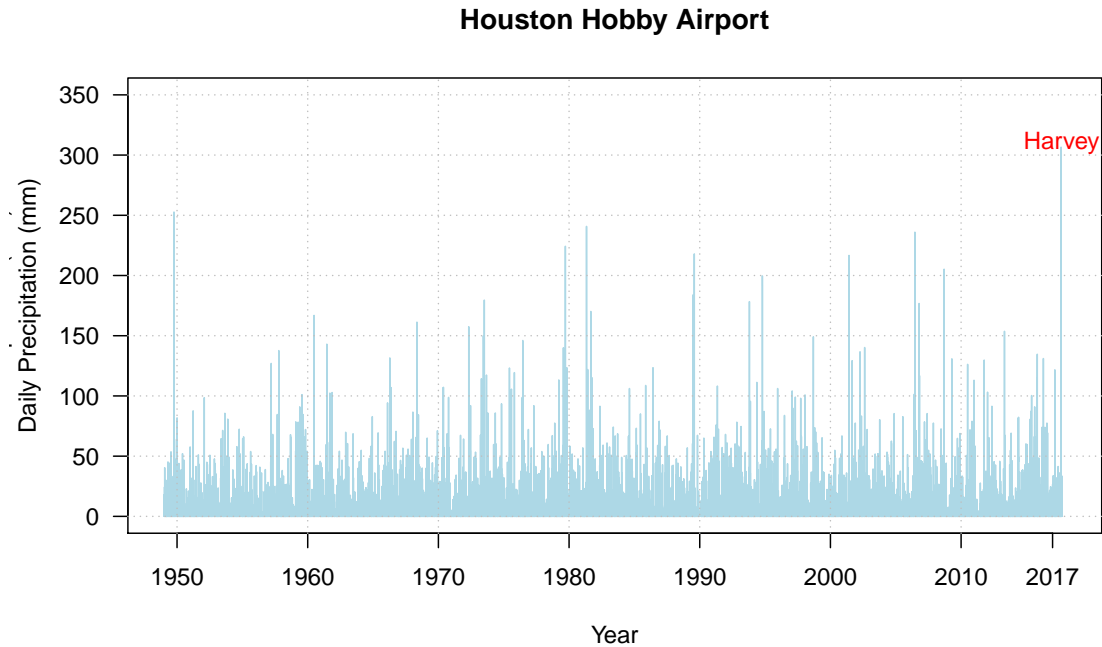


Figure 8: The time series plot of the Houston Hobby Airport daily precipitation from 1949 to 2017. Three out of five largest daily precipitation were observed during 26th to 28th August, 2017.

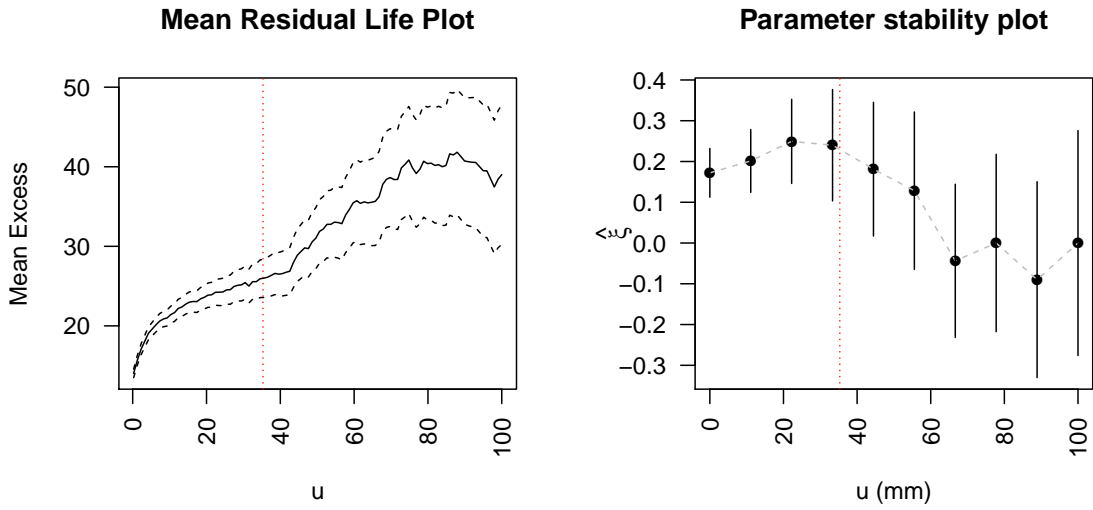


Figure 9: The mean residual life plot and the parameter stability plot (for the shape parameter of GPD) of the Hobby Airport daily rainfall. The red vertical dotted line in each panel is the chosen threshold in this study (.9 empirical quantile). The key point is that it is not that easy to discern “the threshold” using any of these diagnostic plot.

An important practical issue when applying the LHSpline is that the discretization of

rainfall measurement (in a $1/100^{\text{th}}$ of an inch) introduces an artifact in the finely binned histogram in the log scale (see Fig. 10, left panel) and hence the cross validation choice for λ is affected by this discretization. Almost all the precipitation measurements have precision limit and thus it is important to take this fact into account. Here we try two different values ($\exp(1)$ and $\exp(1.25)$) and truncate the values below to alleviate this “discreteness” effect.

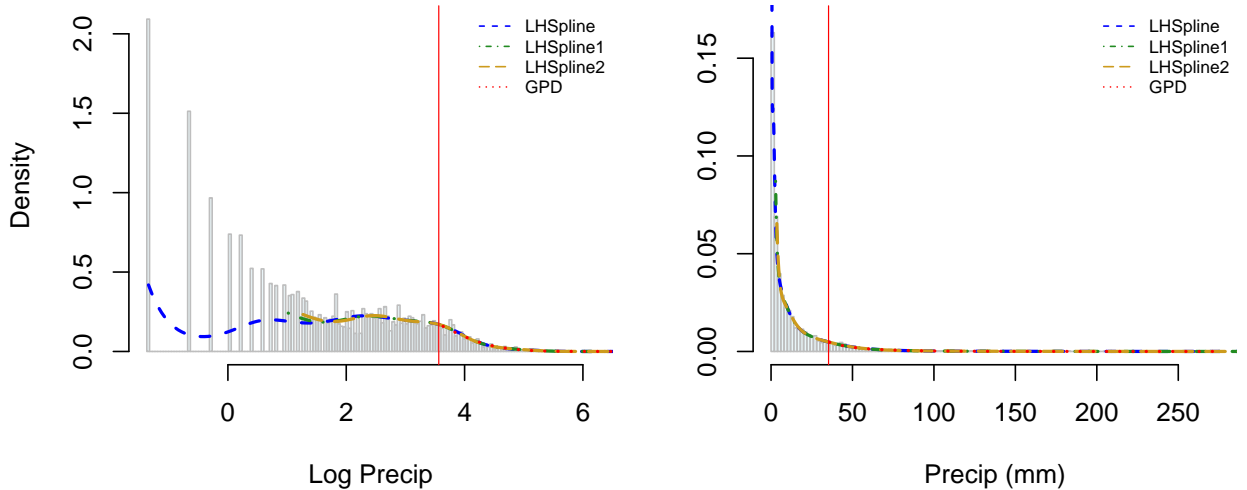


Figure 10: The density estimate for log scale (**left**) and original scale (**right**) of the Hobby airport daily precipitation. The blue dashed lines are the estimates obtained by LH-Spline, green dotdash by LH-Spline with lower bound 1 ($\exp(1)$), golden longdash by LH-Spline with lower bound 1.25 ($\exp(1.25)$), red dotted by POT. The red vertical lines indicate the threshold in the log scale (left) and the original scale (right). The “discreteness” in the log scale is due to the precipitation measurement precision.

As has been demonstrated in Fig. 3 and Fig. 4 in Sec. 3, a good visual agreement in log-density (density) does not necessarily imply that it actually provides a good return level estimate. Fig. 11 shows the estimated log-log plot and return levels ranging from 20 years to 100 years (under the stationary assumption). The LH-Spline give somewhat lower estimates than that of the estimates obtained by POT method. A quantile-quantile plot in Fig. 12 indicates that there might be an issue of overestimating extreme high quantiles in the GPD fit. That is, the GPD estimate of the 68-year rainfall is 337.74 mm whereas the LH-spline estimates (with lower bound 0.254, $\exp(1)$, and $\exp(1.25)$) are 260.39 mm, 267.50 mm, and 270.86 mm, respectively, which are much closer to the maximum value

(252.73 mm) during the 1949 \sim 2016 period. However, one should be aware that the sample maximum can be quite variable and hence might not reflect the true magnitude of the “68-year rainfall”.

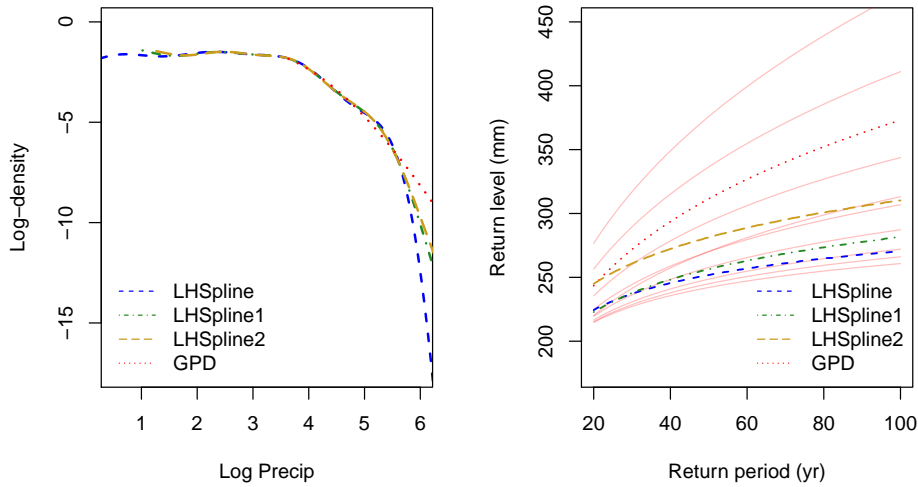


Figure 11: The estimated log densities in the log scale (**left**) and return levels (**right**). Light red lines are POT estimates with different thresholds ranging from .75 to .99 empirical quantile.

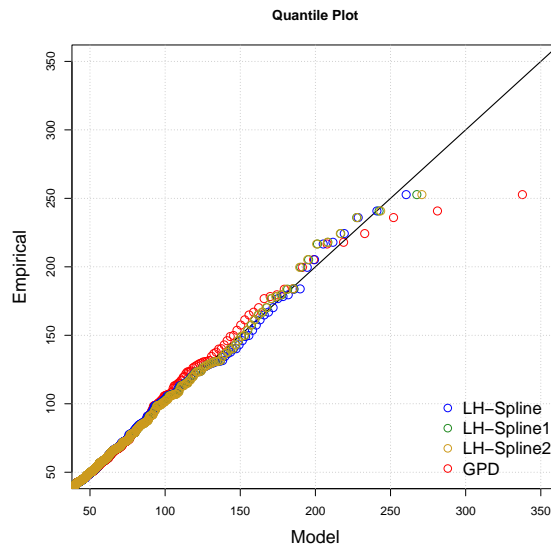


Figure 12: The quantile-quantile plot of the Hobby daily precipitation data (upper 5% of rainy data, those above ~ 50 mm).

Lastly, we would like to investigate the question: “*How unusual was the event of 306.58 mm (26th August, 2017) in daily total precipitation at Hobby Airport?*” To simplify the matter we make a stationarity assumption, that is, the distribution of daily precipitation does not change during the time period 1949 ∼ 2017. The estimates for the return period of the this event are given in the following table:

Table 1: The estimated return period of the 26th August, 2017 daily total precipitation observed at Hobby Airport using POT, LH-Spline method.

Method	POT	LH-Spline	LH-Spline1	LH-Spline2
Estimate (years)	47.07	449.06	196.72	162.09

The much shorter return period estimate obtained from the POT method is due to the overestimation of the upper tail (see Fig. 12) whereas the couple hundred years return period estimated by LH-Splines might be more aligned with what people would expect. Although again one should be aware that there exists, among other issues, a large estimation uncertainty with respect to large return periods.

5 Discussion

In this paper we present the Log-Histospline (LHSpline) method for estimating extreme quantiles of heavy-tailed distributions. The popular EVT based methods require extracting “extreme” observations to fit a corresponding asymptotically justified distribution and then proceed for the tail inference. On the other hand, the LHSpline method makes use of the *full range* of the observations. By combining with data transform and spline smoothing, we have effectively achieved the desirable tail structure that is compatible with what EVT would suggest. We demonstrate through simulation that this method has a potential to provide more precise estimates for return levels with an additional benefit that it jointly model the bulk and the tail of a distribution.

However, by construction, the LHSpline method is only applicable for heavy-tailed distribution, which excludes many important environmental processes, for example, air surface temperature in which may have a bounded tail (Gilleland and Katz, 2006). In terms of implementation, the LHSpline requires some additional tuning, for example, the number of bins for the histogram should grow with the sample size. Limited experiments (not reported here) suggest the estimate is not sensitive to the number of bins once the binning is chosen fine enough. Another tuning issue is to decide how many bins one should extend beyond the range of the observations to remove the boundary effect. Here we suggest increasing the bin range so that the resulting estimate is consistent with the observed maximum and minimum in the data Sec. 2. This choice is in place of picking the threshold in the POT approach and we believe it has less subjectivity.

The theoretical properties of our method is largely unexplored. Much of the theoretical results developed in nonparametric density estimation concern about the performance in terms of global indices such as $\mathbb{E} \left[\int_{x \in \mathbb{R}} |f(x) - \hat{f}(x)| dx \right]$ or $\mathbb{E} \left[\sup_{x \in \mathbb{R}} |f(x) - \hat{f}(x)| \right]$ and largely confined in bounded region (i.e. $x \in [a, b]$, a and b finite). It is not clear how these results can inform us about the estimation performance for extreme quantiles on a potentially unbounded domain.

The LHSpline can be easily extended to more complicated settings. For example it can be extended to model some aspects of spatial extremes, such as the estimation of return level map in a spatial region, by developing an analogy of Cooley et al. (2007) to LHSpline. Also, by converting a density estimation problem into a regression problem (see e.g. Green, 1994, Chapter 4), we may allow for more flexible modeling. For example, one could introduce covariates to account for seasonality and long term trend.

Applying LHSpline to many observational records or the grid cells of climate model output will result in summaries of the distribution that is well suited for further data min-

ing and analysis. The log-density form is particularly convenient for dimension reduction because linear (additive) projection methods such as principle component analysis make sense in the log space. They would not be as effective on the density functions themselves because positivity may not be preserved and the smaller tail probabilities may be discounted. In general we believe the LHSpline will be a useful tool as climate informatics tackles complex problems of quantifying climate extremes.

References

- A. AghaKouchak, D. Easterling, K. Hsu, S. Schubert, and S. Sorooshian. *Extremes in a changing climate detection, analysis and uncertainty*. Water Science and Technology Library. Springer, Dordrecht ; New York, 2012. ISBN 1283740990.
- A. A. Balkema and L. De Haan. Residual life time at great age. *The Annals of Probability*, 2(5):792–804, October 1974. ISSN 00911798.
- L. I. Boneva, D. Kendall, and I. Stefanov. Spline transformations: Three new diagnostic aids for the statistical data- analyst. *Journal of the Royal Statistical Society. Series B (Methodological)*, 33(1):1–71, January 1971. ISSN 00359246.
- L. D. Brown, A. V. Carter, M. G. Low, and C.-H. Zhang. Equivalence theory for density estimation, poisson processes and gaussian white noise with drift. *The Annals of Statistics*, 32(5):2074–2097, October 2004. ISSN 00905364.
- J. Carreau and Y. Bengio. A hybrid pareto model for asymmetric fat-tailed data: the univariate case. *Extremes*, 12(1):53–76, March 2009. ISSN 1386-1999.
- S. Coles. *An introduction to statistical modeling of extreme values*. Springer series in statistics. Springer, London ; New York, 2001. ISBN 1852334592.
- D. Cooley, D. Nychka, and P. Naveau. Bayesian spatial modeling of extreme precipitation return levels. *Journal of the American Statistical Association*, 102(479):824–840, September 2007. ISSN 0162-1459.
- A. C. Davison. Modelling excesses over high thresholds, with an application. In de Oliveira J.T., editor, *Statistical extremes and applications*, pages 461–482. Springer, Dordrecht, 1984. ISBN 978-90-481-8401-9.
- A. C. Davison and R. L. Smith. Models for exceedances over high thresholds (with discussion). *Journal of the Royal Statistical Society, Series B, Methodological*, 52(3), January 1990. ISSN 0035-9246.
- D. K. Dey and J. Yan. *Extreme value modeling and risk analysis: methods and applications*. Chapman and Hall/CRC, Boca Raton, FL, 2016. ISBN 1498701299.

D. Dupuis. Exceedances over high thresholds: A guide to threshold selection. *Extremes*, 1(3):251–261, January 1999. ISSN 1386-1999.

B. Efron and R. Tibshirani. Using specially designed exponential families for density estimation. *The Annals of Statistics*, 24(6):2431–2461, December 1996. ISSN 00905364.

P. H. Eilers and B. D. Marx. Flexible smoothing with b -splines and penalties. *Statistical Science*, 11(2):89–102, May 1996. ISSN 08834237.

P. Embrechts, C. Klüppelberg, and T. Mikosch. *Modelling extremal events for insurance and finance*. Applications of mathematics ; 33. Springer, New York, 1997. ISBN 3540609318.

A. Frigessi, O. Haug, and H. Rue. A dynamic mixture model for unsupervised tail estimation without threshold selection. *Extremes*, 5(3):219–235, September 2002. ISSN 1386-1999.

A. E. Gelfand and A. F. Smith. Sampling-based approaches to calculating marginal densities. *Journal of the American statistical association*, 85(410):398–409, 1990.

E. Gilleland and R. W. Katz. Analyzing seasonal to interannual extreme weather and climate variability with the extremes toolkit. In *18th Conference on Climate Variability and Change, 86th American Meteorological Society (AMS) Annual Meeting*, volume 29. Citeseer, 2006.

I. J. Good and R. A. Gaskins. Nonparametric roughness penalties for probability densities. *Biometrika*, 58(2):255–277, August 1971. ISSN 00063444.

P. J. P. J. Green. *Nonparametric regression and generalized linear models : a roughness penalty approach*. Monographs on statistics and applied probability (Series) ; 58. Chapman and Hall, London ; New York, 1st ed.. edition, 1994. ISBN 0412300400.

C. Gu. *Smoothing spline ANOVA models*. Springer series in statistics, 297. Springer, New York, 2nd ed.. edition, 2013. ISBN 1299337511.

E. J. Gumbel. *Statistics of extremes*. Columbia University Press, New York, 1958. ISBN 0231021909.

W. K. Huang, M. L. Stein, D. J. McInerney, S. Sun, and E. J. Moyer. Estimating changes in temperature extremes from millennial-scale climate simulations using generalized extreme value (GEV) distributions. *Advances in Statistical Climatology, Meteorology and Oceanography*, 2(1), July 2016. ISSN 2364-3587.

A. F. Jenkinson. The frequency distribution of the annual maximum (or minimum) values of meteorological elements. *Quarterly Journal of the Royal Meteorological Society*, 81(348):158–171, April 1955. ISSN 0035-9009.

R. W. Katz, M. B. Parlange, and P. Naveau. Statistics of extremes in hydrology. *Advances in Water Resources*, 25(8):1287–1304, 2002. ISSN 0309-1708.

V. V. Kharin, F. W. Zwiers, X. Zhang, and G. C. Hegerl. Changes in temperature and precipitation extremes in the IPCC ensemble of global coupled model simulations. *Journal of Climate*, 20(8):1419–1444, 2007.

V. V. Kharin, F. W. Zwiers, X. Zhang, and M. F. Wehner. Changes in temperature and precipitation extremes in the CMIP5 ensemble. *Climatic Change*, 119(2):345–357, July 2013. ISSN 0165-0009.

C. Kooperberg and C. J. Stone. A study of logspline density estimation. *Computational Statistics and Data Analysis*, 12(3):327–347, 1991. ISSN 0167-9473.

T. Leonard. Density estimation, stochastic processes and prior information. *Journal of the Royal Statistical Society. Series B (Methodological)*, 40(2):113–146, January 1978. ISSN 00359246.

J. K. Lindsey. Comparison of probability distributions. *Journal of the Royal Statistical Society. Series B (Methodological)*, 36(1):38–47, January 1974a. ISSN 00359246.

J. K. Lindsey. Construction and comparison of statistical models. *Journal of the Royal Statistical Society. Series B (Methodological)*, 36(3):418–425, January 1974b. ISSN 00359246.

L. O. Mearns, W. Gutowski, R. Jones, R. Leung, S. McGinnis, A. Nunes, and Y. Qian. A regional climate change assessment program for north america. *Eos, Transactions American Geophysical Union*, 90(36):311–311, September 2009. ISSN 0096-3941.

P. Naveau, R. Huser, P. Ribereau, and A. Hannart. Modeling jointly low, moderate, and heavy rainfall intensities without a threshold selection. *Water Resources Research*, 52(4):2753–2769, April 2016. ISSN 0043-1397.

I. Papastathopoulos and J. A. Tawn. Extended generalised pareto models for tail estimation. *Journal of Statistical Planning and Inference*, 143(1):131–143, January 2013. ISSN 0378-3758.

J. Pickands. Statistical inference using extreme order statistics. *The Annals of Statistics*, 3(1):119–131, January 1975. ISSN 00905364.

M. D. Risser and M. F. Wehner. Attributable human-induced changes in the likelihood and magnitude of the observed extreme precipitation during hurricane harvey. *Geophysical Research Letters*, 44(24):12,457–12,464, December 2017. ISSN 0094-8276.

C. Scarrott and A. MacDonald. A review of extreme value threshold estimation and uncertainty quantification. *REVSTAT–Statistical Journal*, 10(1), March 2012. ISSN 1645-6726.

B. A. Shaby and B. J. Reich. Bayesian spatial extreme value analysis to assess the changing risk of concurrent high temperatures across large portions of european cropland. *Environmetrics*, 23(8):638–648, 2012.

B. W. Silverman. On the estimation of a probability density function by the maximum penalized likelihood method. *The Annals of Statistics*, 10(3):795–810, September 1982. ISSN 00905364.

B. W. Silverman. *Density estimation for statistics and data analysis*. Monographs on statistics and applied probability (Series). Chapman and Hall, London ; New York, 1986. ISBN 0412246201.

R. L. Smith. Threshold methods for sample extremes. In de Oliveira J.T., editor, *Statistical Extremes and Applications*, pages 621–638. Springer, Dordrecht, 1984. ISBN 978-90-481-8401-9.

A. Tancredi, C. Anderson, and A. O'Hagan. Accounting for threshold uncertainty in extreme value estimation. *Extremes*, 9(2):87–106, June 2006. ISSN 1386-1999.

R. A. Tapia. *Nonparametric probability density estimation*. Johns Hopkins series in the mathematical sciences ; 1. Johns Hopkins University Press, Baltimore, 1978. ISBN 0801820316.

F. O'Sullivan. Fast computation of fully automated log-density and log-hazard estimators. *SIAM Journal on Scientific and Statistical Computing*, 9(2):363–379, 1988. ISSN 0196-5204.

J. L. Wadsworth and J. A. Tawn. Likelihood-based procedures for threshold diagnostics and uncertainty in extreme value modelling. *Journal of the Royal Statistical Society: Series B (Statistical Methodology)*, 74(3):543–567, June 2012. ISSN 1369-7412.

G. Wahba. *Spline models for observational data*. CBMS-NSF Regional Conference series in applied mathematics ; 59. Society for Industrial and Applied Mathematics (SIAM, 3600 Market Street, Floor 6, Philadelphia, PA 19104), Philadelphia, Pa., 1990. ISBN 0898712440.

M. P. Wand, J. S. Marron, and D. Ruppert. Transformations in density estimation. 86(414):343–353, June 1991. ISSN 0162-1459.

J. Wang and V. R. Kotamarthi. High-resolution dynamically downscaled projections of precipitation in the mid and late 21st century over north america. *Earth's Future*, 3(7):268–288, 2015. ISSN 2328-4277. 2015EF000304.

F. W. Zwiers and V. V. Kharin. Changes in the extremes of the climate simulated by CCC GCM2 under CO₂ doubling. *Journal of Climate*, 11(9):2200–2222, 1998. ISSN 0894-8755.